

# Brachial plexus assessment with three-dimensional isotropic resolution fast spin echo MRI: comparison with conventional MRI at 3.0 T

<sup>1</sup>A TAGLIAFICO, MD, <sup>2</sup>G SUCCIO, MD, <sup>1</sup>C E NEUMAIER, MD, <sup>1</sup>G BAILO, MD, <sup>2</sup>G SERAFINI, MD, <sup>2</sup>M GHIDARA, MD, <sup>1</sup>M CALABRESE, MD and <sup>3</sup>C MARTINOLI, MD

<sup>1</sup>National Institute for Cancer Research, Department of Radiology, Genoa, Italy, <sup>2</sup>Radiology Department, Santa Corona Hospital, Savona, Italy, and <sup>3</sup>Radiology Department, University of Genova, Genoa, Italy

**Objective:** The purpose of our study was to determine whether a three-dimensional (3D) isotropic resolution fast spin echo sequence (FSE-cube) has similar image quality and diagnostic performance to a routine MRI protocol for brachial plexus evaluation in volunteers and symptomatic patients at 3.0 T. Institutional review board approval and written informed consent were guaranteed.

**Methods:** In this prospective study FSE-cube was added to the standard brachial plexus examination protocol in eight patients (mean age, 50.2 years) with brachial plexus pathologies and in six volunteers (mean age, 54 years). Nerve visibility, tissue contrast, edge sharpness, image blurring, motion artefact and acquisition time were calculated for FSE-cube sequences and for the standard protocol on a standardised five-point scale. The visibility of brachial plexus nerve and surrounding tissues at four levels (roots, interscalene area, costoclavicular space and axillary level) was assessed.

**Results:** Image quality and nerve visibility did not significantly differ between FSE-cube and the standard protocol ( $p > 0.05$ ). Acquisition time was statistically and clinically significantly shorter with FSE-cube ( $p < 0.05$ ). Pathological findings were seen equally well with FSE-cube and the standard protocol.

**Conclusion:** 3D FSE-cube provided similar image quality in a shorter acquisition time and enabled excellent visualisation of brachial plexus anatomy and pathology in any orientation, regardless of the original scanning plane.

Received 15 June 2010  
Revised 8 September 2010  
Accepted 6 October 2010

DOI: 10.1259/bjr/28972953

© 2012 The British Institute of Radiology

Brachial plexus examination remains difficult because of its particular orientation and it is conventionally realised using sequential multiplanar two-dimensional (2D) sequences with various contrasts such as  $T_1$ ,  $T_2$  and  $T_2$  short tau inversion–recovery (STIR) sequences for fat saturation contrast [1–5]. As a consequence, the acquisition plane is never exactly the right plane to better visualise and analyse the brachial plexus. Three-dimensional (3D) acquisitions allow one either to reconstruct images perpendicular to the plexus or, in double obliquity, to slice through the cords and trunks of the plexus. 3D acquisitions implemented to image the plexus are highly  $T_2$  weighted, like constructive interference in the steady state (CISS)3D, fast imaging with steady-state precession (TrueFISP 3D) or 3D STIR sequences [5–7]. 3D sequences allow a good depiction of compressive nerve root and nerve root avulsions [5]. It has recently been demonstrated that 3D STIR acquisitions are useful for the initial screening of patients with tumoural aetiologies of the brachial plexus. Moreover, they are a valuable adjunct in the detection of space-occupying lesions,

yielding better depiction of nerve site compression and providing a better understanding of the pathophysiology [5]. Moreover, 3D STIR sequences can be used as a high-resolution mask to be fused with fraction of anisotropy maps calculated from diffusion tensor imaging data of the plexus [5].

A recently introduced technique, 3D fast recovery fast spin echo (FRFSE)-cube, uses variable flip angle refocusing, autocalibrating 2D accelerated parallel imaging and non-linear view ordering to produce high-resolution volumetric image sets [8]. The image data, with approximately 0.7 mm isotropic resolution, can be reformatted in any plane, regardless of the prescribed plane during the image acquisition. The cube technique has been shown in various applications and specifically compared with 2D fast spin echo (FSE) for imaging of the knee, ankle, brain and uterus at 1.5 T [8–13]. Advantages of 3D cube sequences include high image quality and good 3D reconstructions in a shorter acquisition time [8,11]. The improved acquisition efficiency of cube sequences allowing data to be reformatted in arbitrary planes is ideal for complex anatomy such as that found at the brachial plexus level.

The purpose of our study was to compare 3D FSE-cube with a standard protocol for brachial plexus imaging using a 3 T system.

Address correspondence to: Dr Alberto Tagliafico, Department of Experimental Medicine—DIMES, University of Genoa, Largo R. Benzi 8, 16132 Genoa, Italy. E-mail: alberto.tagliafico@unige.it

## Methods and materials

### Subjects

The study was approved by the institutional review board and informed consent was obtained from all volunteers and patients.

From November 2009 to May 2010, six volunteers (mean age, 54 years; age range, 19–65 years) and eight patients (mean age, 50.2 years; age range, 25–69 years) with symptoms related to the brachial plexus (dysaesthesia or paraesthesias or motor deficit) were included in this study.

All healthy volunteers were recruited from the hospital staff.

Patients were referred to the MR unit to study the brachial plexus for assessment of nerve tumours (four patients) and brachial plexus involvement following breast cancer (three patients) and trauma (one patient). The diagnosis was confirmed by surgery or by patient follow-up of at least 6 months.

### MRI protocol

All healthy volunteers and all patients underwent both standard three-plane 2D FSE and 3D FSE-cube imaging with and without fat saturation using a 3.0 T MRI system (GE Signa HDxt 3.0 T; GE Healthcare, Little Chalfont, UK).

A 16-channel neurovascular coil was combined with an 8-channel spine coil covering the field of view with 24 coil elements.

The imaging protocols used in this study were the result of a pilot study performed with five healthy volunteers who underwent MRI of the brachial plexus at 3.0 T (A Tagliafico, unpublished data, Genoa, Italy, 2009). In this pilot study, the best combination of acquisition and processing parameters was assessed with regard to image quality and practicability for clinical imaging (Table 1).

The standard imaging protocol included  $T_1$  weighted turbo spin echo (TSE) sequences in the coronal, transverse and sagittal oblique planes and  $T_2$  weighted TSE sequences with fat saturation in the coronal, transverse and sagittal oblique planes.  $T_1$  weighted TSE sequences following gadolinium administration ( $0.1 \text{ mmol kg}^{-1}$  body weight) were obtained in patients when necessary.

The  $T_1$  weighted images were used to display regional anatomy, including the various muscles, blood vessels

and nerves outlined by tissue fat planes. The  $T_2$  weighted images were obtained with fat saturation because abnormal intraneural signal from components of the plexus, such as a root or a cord, may be obscured by adjacent fat signal.

The FSE-cube sequence was performed with a 2D autocalibrating parallel imaging reconstruction technique (ARC; GE Healthcare) with an acceleration factor of three to reduce imaging time. The FSE-cube isotropic source data were used to create sagittal, coronal, axial and oblique reformatted images with 0.5 mm section thickness.

Multiplanar reconstructions were performed using open source software (OsiriX3.6 32-bit; Pixmeo, Geneva Switzerland) using 3D FSE-cube images. Images from data sets were compared in a randomised fashion for image quality by two radiologists with 6 and 8 years of experience in brachial plexus MRI. The radiologists were blinded to the type of sequence analysed.

Nerve visibility, tissue contrast, edge sharpness, image blurring and motion artefact were calculated for FSE-cube sequences and for the standard protocol on a standardised five-point scale.

A score of 1 was considered poor and a score of 5 was considered excellent for tissue contrast and edge sharpness, whereas a score of 1 was considered uninterpretable and a score of 5 indicated no image blurring or motion artefact.

Hence, a higher score is reflective of superior image quality. Overall image quality was assessed on the basis of the mean of all scores. Each reader also classified the degree of diagnostic confidence using a similar scale (1, poor; 5, excellent).

The visibility of the brachial plexus nerve at four anatomic levels (roots, interscalene area, costoclavicular space and axillary level) was evaluated. The following scoring system was used for grading visibility of the different anatomic structures: a score of 1 indicated that the nerve structure was not visible; a score of 2 indicated that a structure was visible but not able to be analysed (*i.e.* MR characteristics could not be interpreted); a score of 3 indicated that a structure was visible and able to be analysed; and a score of 4 indicated that a structure was clearly visible, with sharp outlines. A similar 0–4 grading system was used to compare 2D sequences with 3D FSE-cube sequences in local staging of brachial plexus tumour (vessel infiltration, bone involvement and proximal extension into the spinal canal).

**Table 1.** Parameters for 3D FSE-cube imaging and standard FSE sequences for brachial plexus evaluation

Parameters	3D FSE-cube	2D $T_1$ FSE	2D $T_2$ FSE
TR (ms)	2200	600	2500
TE (ms)	79	25	80
Field of view (cm)	35	35	35
Matrix	$512 \times 512$	$512 \times 512$	$512 \times 512$
Echo-train length	60	12	25
Slice thickness and overlap	0.5, 0.1 overlap	3	3
Scanning plane	Axial	All	All
SAR ( $\text{W kg}^{-1}$ body weight)	0.5	1.2	1.3
Bandwidth ( $\text{Hz px}^{-1}$ )	244	122	134
Scan time (min)	7	4	5

FSE, fast spin echo; SAR, specific absorption rate; TE, echo time; TR, repetition time; 3D, three-dimensional; 2D, two-dimensional.

### Statistical analysis

Wilcoxon's signed ranked test was used for comparison of image quality and nerve visibility for 3D FSE-cube and the standard protocol.  $p$ -values  $<0.05$  were considered statistically significant.

### Results

Every patient and volunteer required an adequate MRI to be included in the study.

In every patient a neurogenic tumour ( $n=4$ ), brachial plexus involvement following breast cancer ( $n=3$ ) and traumatic lesion of the brachial plexus was diagnosed with both standard protocol and FSE-cube (Figures 1–4).

The 3D FSE-cube volumetric data set was acquired in approximately 7 min. In contrast, the acquisition of the three-plane 2D FSE data set required approximately 16 min.

Image quality and brachial plexus nerve visibility were not significantly different between FSE-cube sequences and the standard protocol ( $p>0.05$ ) (Table 2). Local staging for vessel infiltration, bone involvement and proximal extension into the spinal canal did not differ between FSE-cube and the standard protocol ( $p>0.05$ ) (Table 3).

In both volunteers and patients intradural roots and spaces were visualised sufficiently to suspect the possible presence of a traumatic root avulsion (Figure 5). However, 3D FSE-cube sequences appeared not to be adequate to assess and evaluate exhaustively a root avulsion.

### Discussion

Our study demonstrates that high-quality MR neurography of the brachial plexus is possible with 3D FSE-cube sequences using a 3 T system. With these sequences brachial plexus nerves are clearly visualised at different levels from the root level to the axillary level. Using 3D FSE-cube sequences it was easier to analyse the spatial localisation of nerve lesions within and along nerve segments. As demonstrated in a recent study for 3D STIR sequences [5], the anatomical coverage offered by the 3D acquisition guaranteed by FSE-cube sequences and the ability to slice through the volume of interest helped to analyse how the lesion modifies and affects the nerve's course. The use of maximum intensity projection and multiplanar reconstruction may be useful especially in an oncological setting to visualise tumoural bulk and nerve distortion and/or compression.

The use of fat saturation on 3D FSE-cube sequences enables analysis of the bone marrow contrast similarly to 2D FSE  $T_2$  weighted sequences. Moreover, 3D FSE-cube sequences, as for 3D STIR sequences, is useful to evaluate traumatic injuries involving the spinal cord, such as nerve avulsion [5]. However, using 3D FSE-cube sequences, some areas of inhomogeneous fat saturation are visible. This fact may be sufficient to reduce reliability in the evaluation of  $T_2$  signal intensity changes in the nerves of the brachial plexus. However, it is important to remember that  $T_2$  signal intensity may not be sufficiently reliable to identify pathological conditions in peripheral nerves because the signal intensity may

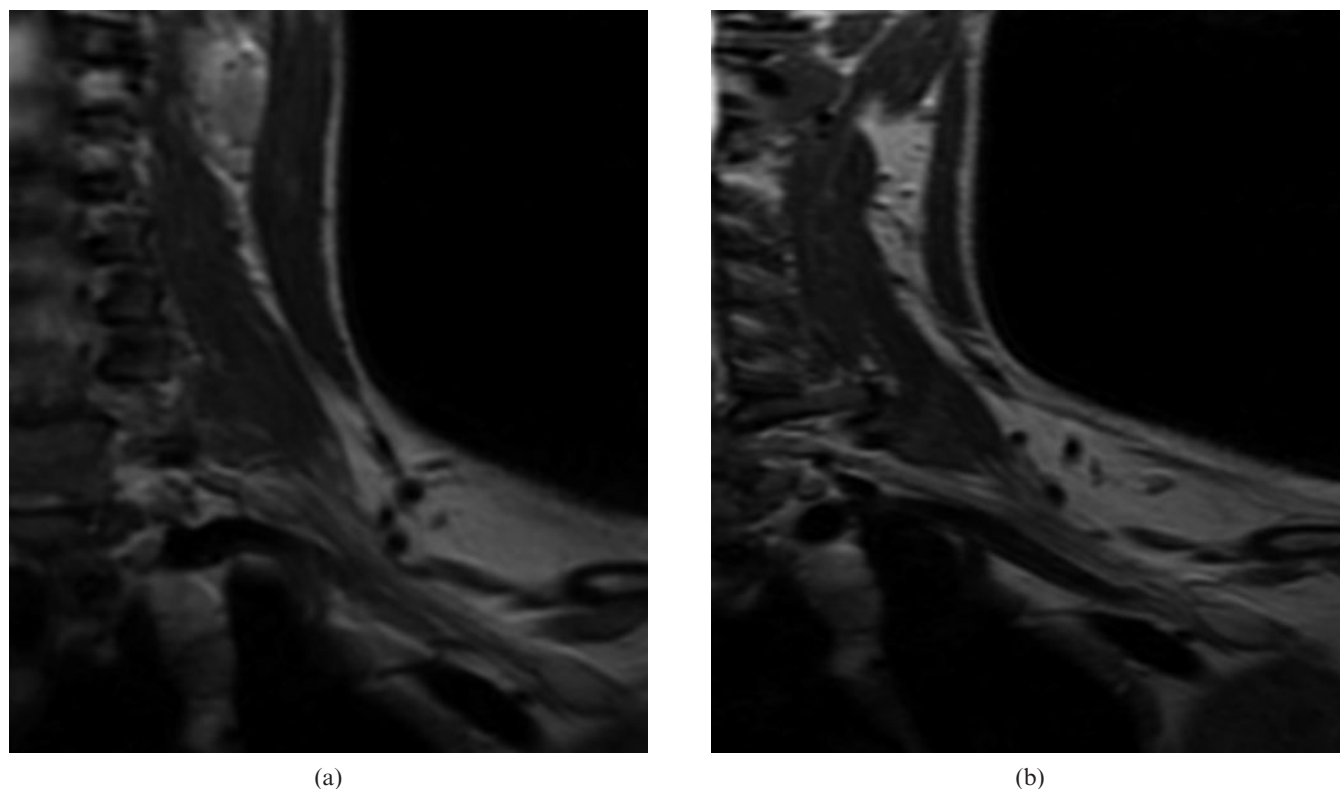


**Figure 1.** Normal control: (a) fast spin echo (FSE)-cube sequence and (b) coronal  $T_2$  weighted turbo spin echo image. Note how the brachial nerve anatomy is well rendered in both acquisitions. Tissue contrasts are comparable for (a) FSE-cube sequences and (b)  $T_2$  weighted sequences.

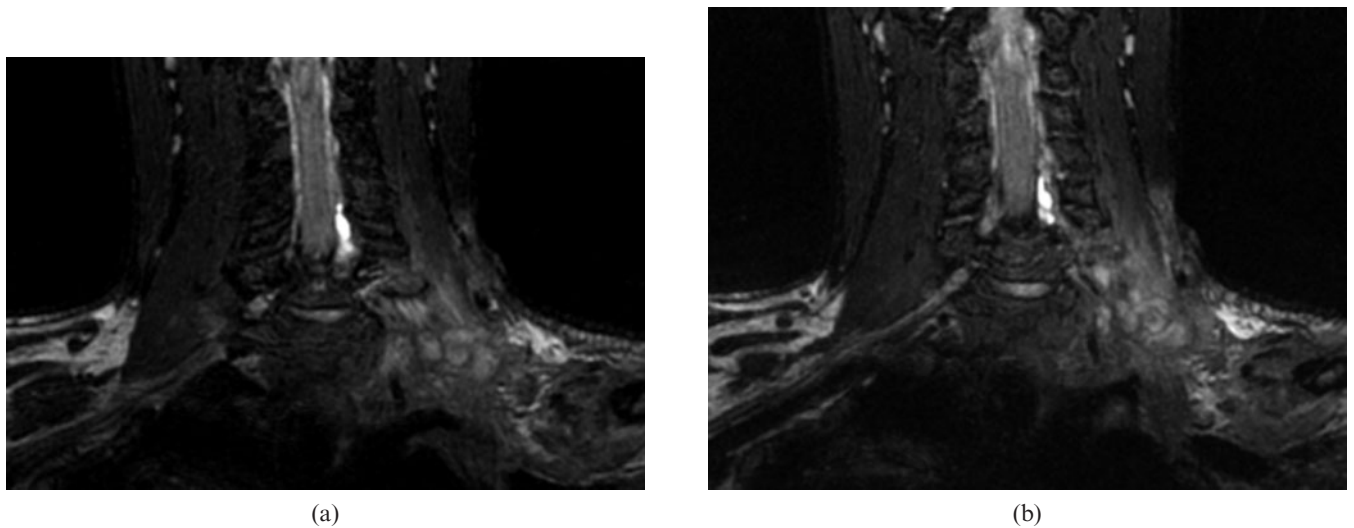


**Figure 2.** (a) Coronal oblique three-dimensional fast spin echo-cube with fat saturation reconstruction of the left brachial plexus shows massive disruption of the brachial plexus in a patient with traumatic injury. (b) Coronal  $T_2$  weighted turbo spin echo image with fat saturation at the same level demonstrates similar findings.

also be increased in asymptomatic subjects [14]. Another possible solution may be to use  $T_2$  weighted sequences with the IDEAL technique (iterative decomposition of water and fat with echo asymmetry and least-squares estimation), which can robustly separate water and fat signals, but inevitably increases scan time, making

separated images more easily affected by patient movement, and loses the advantages of 3D imaging. To reduce patient motion the PROPELLER technique (periodically rotated overlapping parallel lines with enhanced reconstruction) and turboprop technique offer an effective approach to correct for motion artefacts [15].

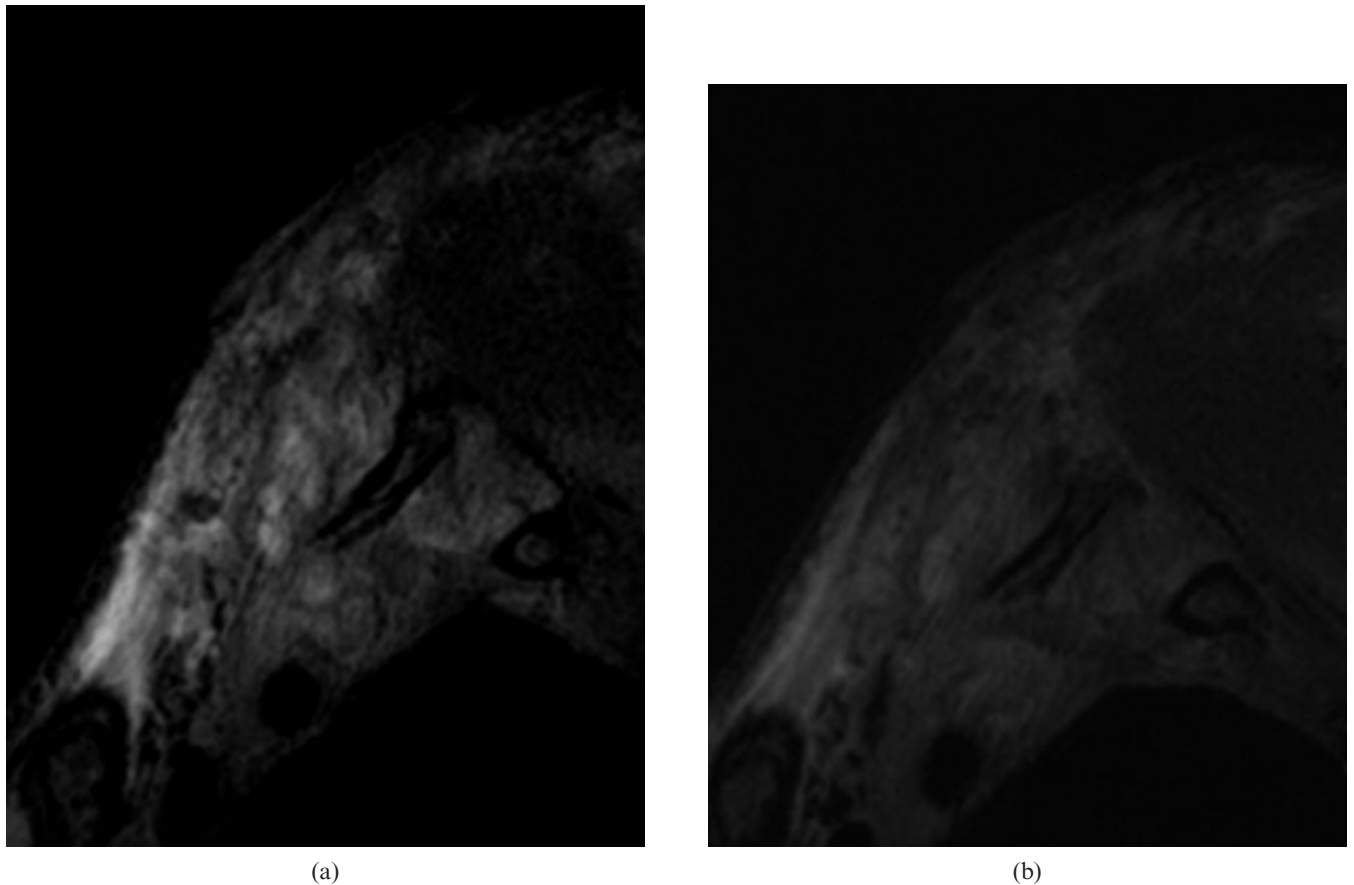


**Figure 3.** (a) Sagittal oblique three-dimensional fast spin echo-cube with fat saturation view of the left brachial plexus shows terminal neuromas in a patient with traumatic injury. (b) Sagittal  $T_2$  weighted turbo spin echo image with fat saturation at the same level demonstrates neuromas as well.

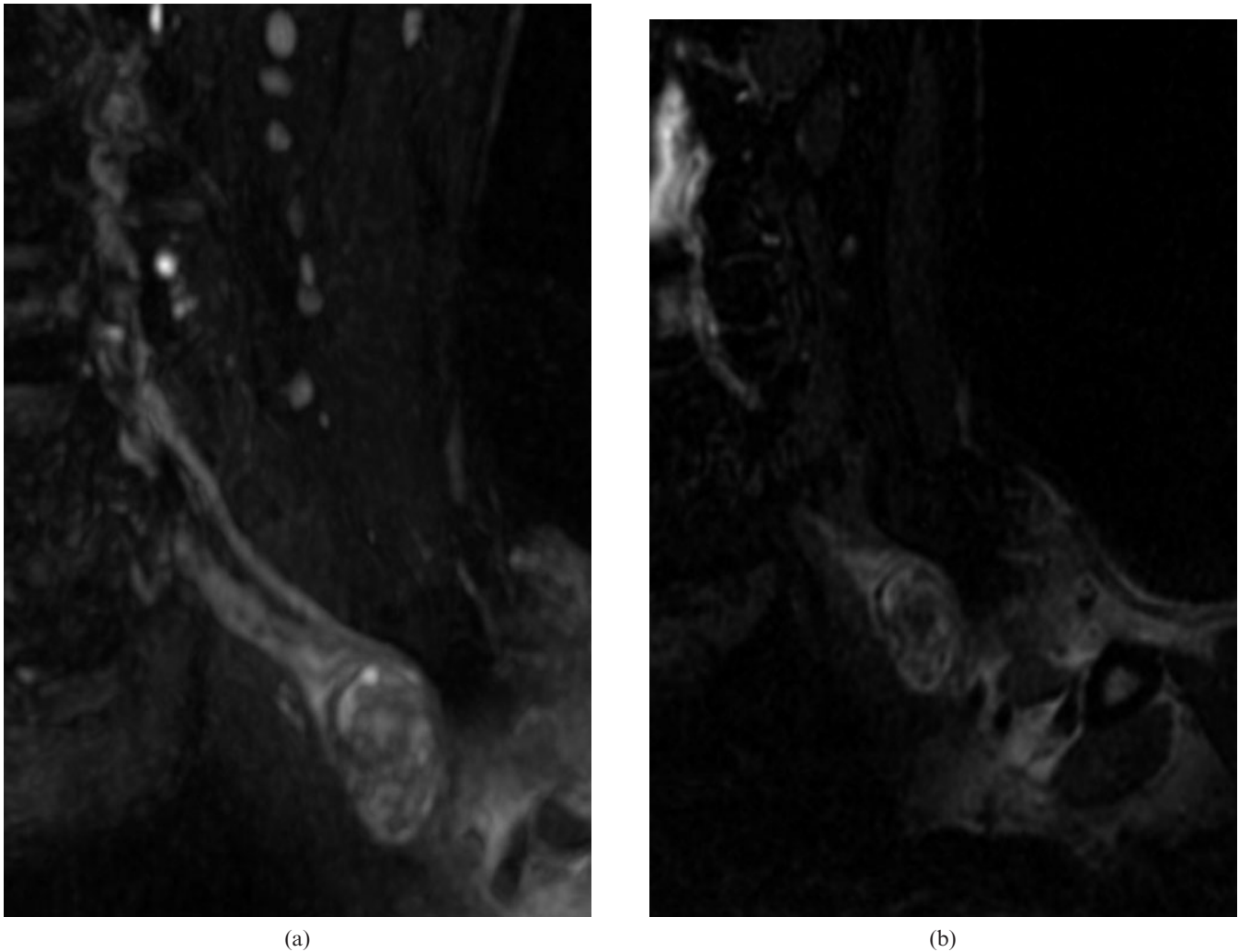


**Figure 4.** A 43-year-old patient with suspected brachial plexus schwannoma. MR images confirm the diagnosis. Detection and delineation of the tumour as well as tissue contrasts are comparable for (a) fast spin echo-cube and (b)  $T_2$  weighted sequences with fat saturation.

In our study image quality and nerve visibility were scored equally well on both the standard protocol and 3D FSE-cube sequences. These data are different from a recent study in which 3D FRFSE-cube provided superior image quality to 2D FRFSE sequences at the level of the uterus using a 1.5T system [8]. The reason for this difference may be explained by the use of 3 T equipment in our study and by the use of FSE sequences instead of FRFSE sequences. However, in our study pathological findings were seen equally well with both protocols. In the literature the use of 3D FRFSE-cube sequences despite an improved image quality did not improve diagnostic confidence compared with standard protocols

[8]. The use of 3D FSE-cube sequences at the knee yielded similar diagnostic performance to a routine MRI protocol at 3.0 T [13]. We believe the 3D FSE-cube can be used to provide rapid comprehensive brachial plexus assessment especially in patients with severe pain or claustrophobia who cannot tolerate a 20 min routine MRI examination. This is particularly important in patients with neurological disturbances due to trauma or tumoural involvement of brachial plexus nerves. We acknowledge that additional studies are needed to determine whether 3D FSE-cube can replace currently used 2D sequences for evaluating the brachial plexus in all patients undergoing routine MRI.

**Table 2.** Mean overall image quality and brachial plexus nerve visibility evaluated by two blinded reviewers

Reviewer	Mean overall image quality			Mean nerve visibility		
	3D FSE Cube	2D FSE	<i>p</i> -value <sup>a</sup>	3D FSE Cube	2D FSE	<i>p</i> -value <sup>b</sup>
1	3.5 ± 0.7	3.3 ± 0.4	0.65	3.6 ± 0.4	3.5 ± 0.3	0.56
2	3.4 ± 0.6	3.2 ± 0.5	0.83	3.3 ± 0.3	3.4 ± 0.4	0.44

FSE, fast spin echo; 3D, three-dimensional; 2D, two-dimensional.

<sup>a</sup>Scoring on a five-point scale.

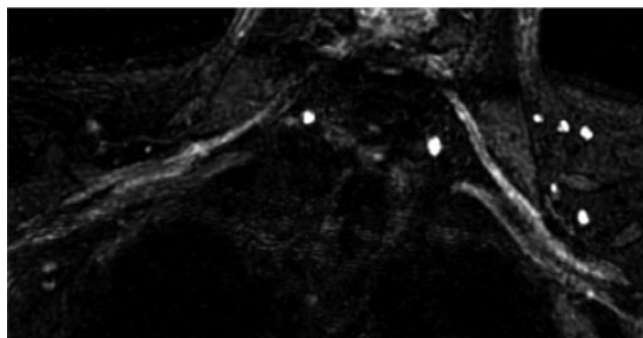
<sup>b</sup>Scoring on a four-point scale.

**Table 3.** Mean visibility evaluated by two blinded reviewers of vessel infiltration, bone involvement and proximal extension into the spinal canal of the tumour for local staging

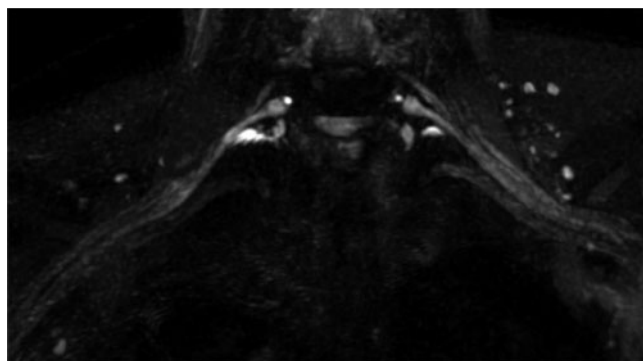
Reviewer	3D FSE-cube	2D FSE	p-value
1	3.4 ± 0.2	3.2 ± 0.1	0.32
2	3.8 ± 0.2	3.7 ± 0.2	0.81

FSE, fast spin echo; 3D, three-dimensional; 2D, two-dimensional. Scoring on a four-point scale.

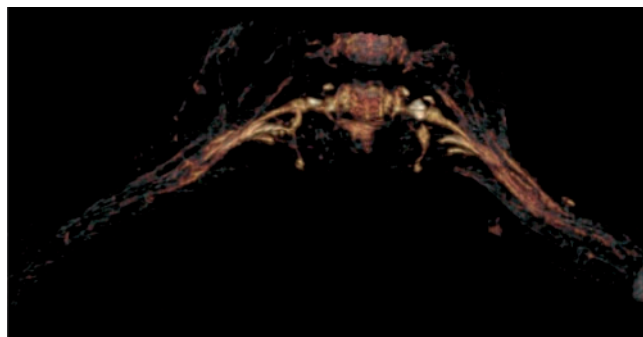
Our study had several limitations. One limitation was our small patient population. Many of the *p*-values in our study comparing FSE-cube and the routine MRI protocol that were not statistically significant may change if



(a)



(b)



(c)

**Figure 5.** Demonstration of brachial plexus fibres on a normal volunteer. Images are acquired with three-dimensional fast spin echo-cube with fat saturation. (a) The normal brachial plexus depicted on native images. (b) Fibres have been reconstructed using a multiplanar reconstruction algorithm. (c) Fibres are visualised in false colours using a volume rendering algorithm. Note that visualisation of roots is possible but not accurate.

additional clinical studies are considered. However, it is possible that achieving a statistically significant difference may not be clinically relevant since all pathologies were seen well with both protocols.

Another limitation was the presence of a selection bias because our study group consisted of only a proportion of all patients undergoing routine MRI of the brachial plexus at our institution. Another limitation was that intradural roots and spaces were visualised sufficiently to suspect the presence of a traumatic root avulsion but not to assess adequately and evaluate exhaustively a root avulsion. For intradural root avulsion evaluations different sequences should be used.

Compared with the standard protocol, 3D FSE-cube provides similar image quality in a shorter acquisition time and enables excellent visualisation of brachial plexus anatomy in any orientation, regardless of the original scanning plane.

3D FSE-cube eliminates the need for multiple-plane 2D acquisition, thus decreasing the time required to obtain the images. This is extremely useful in patients with severe pain or claustrophobia.

## References

1. Aagaard BD, Maravilla KR, Kliot M. MR neurography MR imaging of peripheral nerves. *Magn Reson Imaging Clin N Am* 1998;6:179–94.
2. Kim S, Choi JY, Huh YM, Song HT, Lee SA, Kim SM, et al. Role of magnetic resonance imaging in entrapment and compressive neuropathy—what, where, and how to see the peripheral nerves on the musculoskeletal magnetic resonance image: part 2. Upper extremity. *Eur Radiol* 2007;17:509–22.
3. Todd M, Shah GV, Mukherji SK. MR imaging of brachial plexus. *Top Magn Reson Imaging* 2004;15:113–25.
4. van Es HW. MRI of the brachial plexus. *Eur Radiol* 2001;11:325–36.
5. Viallon M, Vargas MI, Jlassi H, Lövblad KO, Delavelle J. High-resolution and functional magnetic resonance imaging of the brachial plexus using an isotropic 3D T<sub>2</sub> STIR (short term inversion recovery) SPACE sequence and diffusion tensor imaging. *Eur Radiol* 2008;18:1018–23.
6. Gasparotti R, Ferraresi S, Pinelli L, Crispino M, Pavia M, Bonetti M, et al. Three-dimensional MR myelography of traumatic injuries of the brachial plexus. *AJNR Am J Neuroradiol* 1997;18:1733–42.
7. Vargas MI, Delavelle J, Jlassi H, Rilliet B, Viallon M, Becker CD, et al. Clinical applications of diffusion tensor tractography of the spinal cord. *Neuroradiology* 2008;50:25–9.
8. Agrawal G, Riherd JM, Busse RF, Hinshaw JL, Sadowski EA. Evaluation of uterine anomalies: 3D FRFSE cube versus standard 2D FRFSE. *AJR Am J Roentgenol* 2009;193:W558–62.
9. Busse RF, Brau AC, Vu A, Michelich CR, Bayram E, Kijowski R, et al. Effects of refocusing flip angle modulation and view ordering in 3D fast spin echo. *Magn Reson Med* 2008;60:640–9.
10. Gold GE, Busse RF, Beehler C, Han E, Brau AC, Beatty PJ, et al. Isotropic MRI of the knee with 3D fast spin echo extended

- echo-train acquisition (XETA): initial experience. *AJR Am J Roentgenol* 2007;188:1287–93.
11. Stevens K, Busse RF, Han E, Brau AC, Beatty PJ, Beaulieu CF, et al. Ankle: isotropic MR imaging with 3D-FSE cube—initial experience with healthy volunteers. *Radiology* 2008;249:1026–33.
  12. Ghagla GH, Busse RF, Syndor R, Rowley HA, Turski P. Three-dimensional fluid-attenuated inversion recovery imaging with isotropic resolution and nonselective adiabatic inversion provides improved three-dimensional visualization and cerebrospinal fluid suppression compared to 2D FLAIR at 3 tesla. *Invest Radiol* 2008;43:547–51.
  13. Kijowski R, Davis KW, Woods MA, Lindstrom MJ, De Smet AA, Gold GE, et al. Knee joint: comprehensive assessment with 3D isotropic resolution fast spin echo MR imaging—diagnostic performance compared with that of conventional MR imaging at 3.0 T. *Radiology* 2009;252:486–95.
  14. Husarik DB, Saupe N, Pfirmann CW, Jost B, Hodler J, Zanetti M. Elbow nerves: MR findings in 60 asymptomatic subjects—normal anatomy, variants, and pitfalls. *Radiology* 2009;252:148–56.
  15. Huo D, Li Z, Aboussouan E, Karis JP, Pipe JG. Turboprop IDEAL: a motion-resistant fat-water separation technique. *Magn Reson Med* 2009;61:188–95.